Adv. Space Res. Vol.4, No.7, pp.61-70, 1984
Printed in Great Britain.
0273-1177/84 $0.00 + .50

RELATIONSHIPS OF A GROWING MAGNETIC FLUX REGION TO FLARES

S. F. Martin,[1] R. D. Bentley,[2] A. Schadee,[3]
A. Antalova,[4] A. Kucera,[4] L. Dezso",[5] L. Gesztelyi,[5]
K. L. Harvey,[6] H. Jones,[7] S. H. B. Livi[8] and J. Wang[9]

[1]*Solar Astronomy 264–33, California Institute of Technology, Pasadena, CA 91125, U.S.A.*
[2]*Mullard Space Science Laboratory, University College London, Holmburg St. Mary, Dorking, Surrey, England*
[3]*Space Research Laboratory, Beneluxlaan 21, 3527 HS Utrecht, The Netherlands*
[4]*Astronomical Institute Slovak Academy of Sciences, 059 60 Tatranska Lomnica, Czechoslovakia*
[5]*Heliofizikai Obszervatoriuma, Magyar Tudomanyos Akademia, H-4010 Debrecen, Hungary*
[6]*Solar Physics Research Corporation and Visiting Astronomer, National Solar Observatories, Tucson, AZ, U.S.A.*
[7]*NASA/Goddard Space Flight Center and Visiting Astronomer, National Solar Observatories, Tucson, AZ, U.S.A.*
[8]*Instituto de Fisica, Universidade Federal do Rio Grande do Sul, 90000 Porto Alegre, Brazil*
[9]*Beijing Observatory, Academia Sinica, Beijing, People's Republic of China*

ABSTRACT

Some sites for solar flares are known to develop where new magnetic flux emerges and becomes abutted against opposite polarity pre-existing magnetic flux (review by Gaizauskas/1/). We have identified and analyzed the evolution of such flare sites at the boundaries of a major new and growing magnetic flux region within a complex of active regions, Hale No. 16918. This analysis was done as a part of a continuing study of the circumstances associated with flares in Hale Region 16918, which was designated as an FBS target during the interval 18 - 23 June 1980. We studied the initiation and development of both major and minor flares in Hα images in relation to the identified potential flare sites at the boundaries of the growing flux region and to the general development of the new flux. This study lead to our recognition of a spectrum of possible relationships of growing flux regions to flares as follows: (1) intimate interaction with adjacent old flux - flare sites centered at new/old flux boundary, (2) forced or "intimidated" interaction in which new flux pushes old field having lower flux density towards a neighboring old polarity inversion line where a flare then takes place, (3) "influential" interaction - magnetic lines of force over an old polarity inversion line, typically containing a filament, reconnect to the new emerging flux; a flare occurs with erupting filament when the magnetic field overlying the filament becomes too weak to prevent its eruption, (4) inconsequential interaction - new flux region is too small or has wrong orientation for creating flare conditions, (5) incidental - flare occurs without any significant relationship to new flux regions.

INTRODUCTION

Many studies in recent years claim or suggest a relationship between emerging magnetic flux regions and solar flares (reviews by Gaizauskas/1/ and Priest/2/). In most cases the references are not to isolated magnetic flux regions (active regions) but to the development of new magnetic flux within pre-existing active regions. One of our goals in the continuing study of FBS target, Hale Region 16918 has been to investigate and clarify the nature of this relationship between newly developing magnetic flux and the occurrence of flares. In the previous work (Martin et al./3/), we found a statistical relationship between the sites of 66% of the flares and the sites of 17 new magnetic flux regions observed over a period of 8 days. Because the statistical study leaves many questions unanswered about the physical circumstances of the association, we take a different approach in the present work. We investigate in detail how the new magnetic flux regions interact with the magnetic field of the pre-existing active region and then study where the flares occur and where they do not occur in relation to the interaction of the new and old magnetic field. The day to day evolution of Hα, magnetic field, and velocity field data in this complex as a whole, without regard to the sites of new magnetic flux, has been described by Athay, Jones and Zirin/4/.

THE IDENTITY OF A NEW FLUX REGION

In this paper we show the details of only the largest new magnetic flux region, designated as region F in the previous paper (Martin et al./3/). Figure 1 depicts the daily growth of the new flux region in Hα. The new region is first seen on 19 June very near the polarity inversion line of the pre-existing complex of active regions. (See Gaizauskas/5/ for the previous evolution of the complex.) The approximate boundaries of the new flux region are shown by a combination of solid and dashed lines. The solid lines show the sites where part of the new magnetic flux is abutted against opposite polarity flux of the pre-existing active region. At these sites, the boundaries of the new region are very definite and are often clearly marked by filaments. The arrows in Figure 1 indicate that these are also key sites for the initiation of many flares. The dashed sections of line show only the approximate location where new and old magnetic flux of the same polarity have merged. At these places, no definite boundary exists that can be followed from day to day because the magnetic fields of similar polarity intermingle and leave no trace of their previous migration.

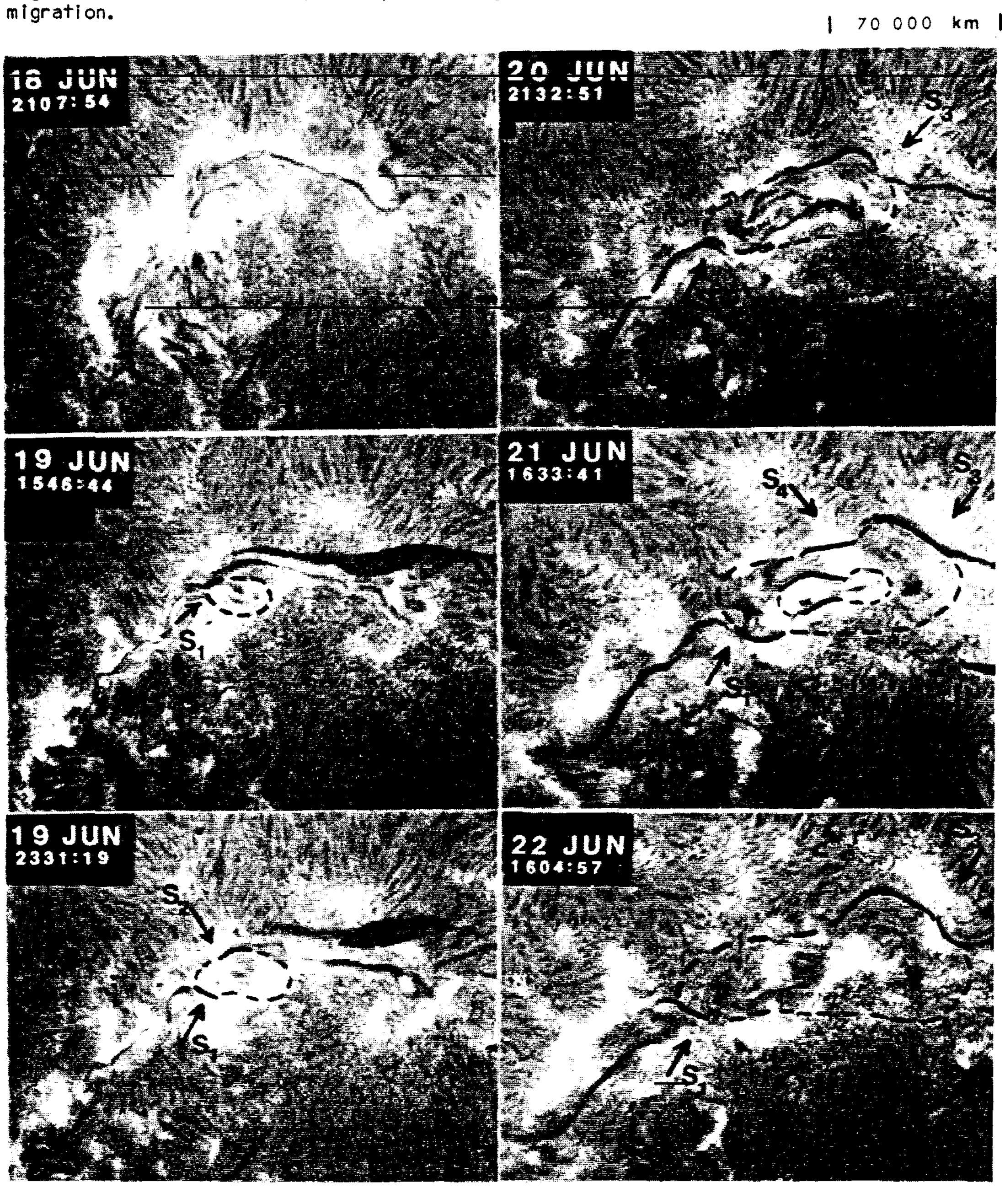

Fig. 1. Photographed in Hα at Big Bear Solar Observatory. The major new flux region developing in an active region complex is outlined by dashed lines and key flare sites at the boundary of this region are labeled S_1, S_2, S_3, and S_4.

We note that this secondary emergence of new flux has all of the same properties of any new active region that could occur on the quiet sun. During the first day it reveals the characteristic arch filament system (Bruzek/6/; Weart/8/) and sunspots. The sunspot evolution is illustrated in Figure 2.

THE IDENTITY OF KEY FLARE SITES

Early on 19 June, there is only one key flare site, S_1 in Figure 1, specifically on the boundary of the new flux region. However, by the end of 19 June, a second potential flare site, S_2, has developed. The second flare site becomes insignificant by 20 June and a third site, S_3, has developed due to the westward growth of the new magnetic flux and concurrent westward motion of sunspot 1.1 in Figure 2. On 21 June, a fourth key flare site develops after the secondary emergence of a small new flux region within the large new flux region. Most of the key flare sites on the boundary of the major new flux region are recognizable by bright plage separated only by a thin filament. Sometimes the filament is broken exactly where the plages of opposite polarity are close together. In all of the key flare sites marked by arrows in Figure 1, compression of the magnetic field along the polarity inversion line occurs and is due to the growth of the new flux region. We confirm the conclusions of Bumba et al./9/ that compression of fields of opposite polarity is a situation that leads to high flare incidence.

Another situation that leads to high flare incidence was described by Martres et al./10/. This is the circumstance of "evolving magnetic features" in which an increase in magnetic flux occurs on one side of a polarity inversion line while a decrease occurs in the adjacent opposite polarity field. This condition of evolving magnetic features is more obvious when we analyze the associated sunspot growth and decay patterns. In Figure 2 the birth of the sunspot group of the new flux region is seen on 19 June, and by 20 June, the spots of the new region already contain the highest flux within the complex. Concurrent with this rapid spot growth, the nearby pre-existing spots, 2.1, 2.11, 2.12 and 2.b, are rapidly disappearing, an important sign of decrease in the total magnetic flux of the old

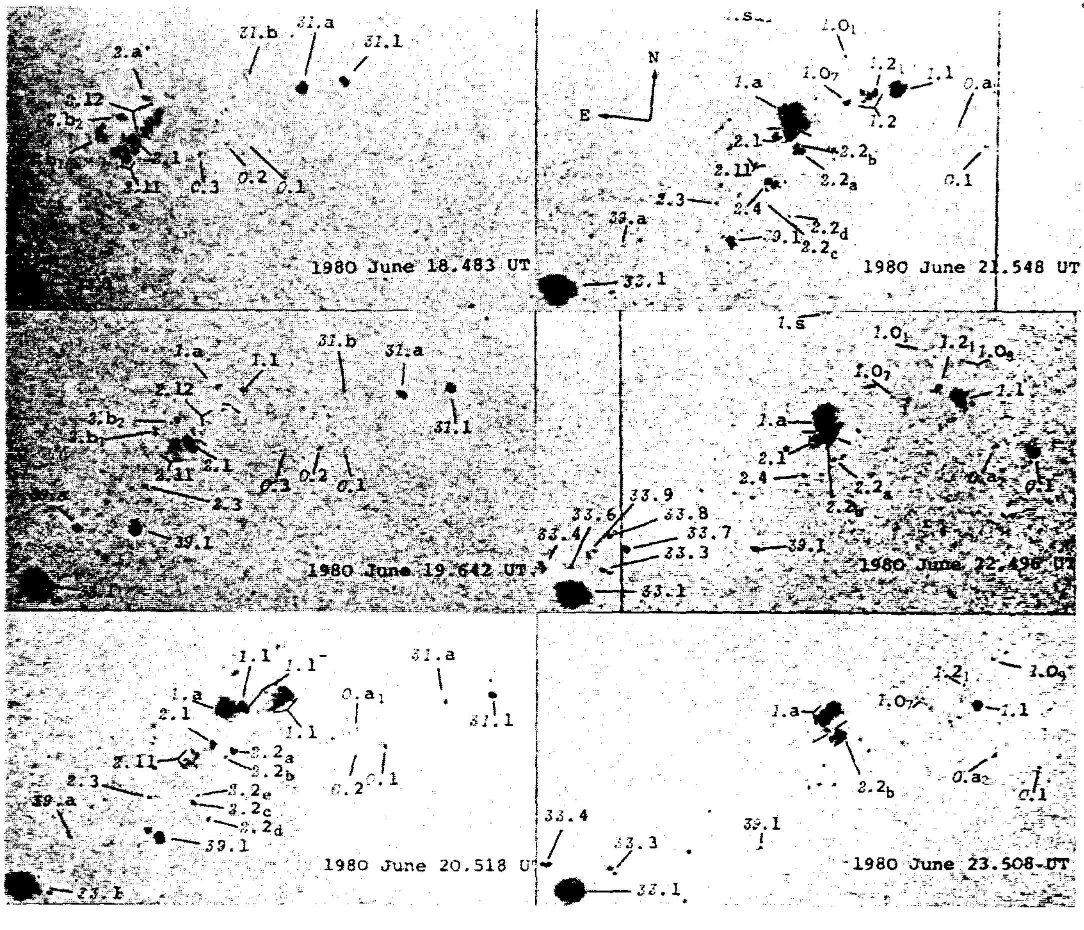

Fig. 2. Photographs from the Debrecen Solar Observatory show the decay of sunspots $2a^+$, 2.12, $2.b_2$, $2.b_1$, 2.1, and 2.11 simultaneously with the growth of spots 1.a and 1.1 and subsequent associated spots of the new flux region illustrated in Figure 1.

flux region. Flare site S_1 lies between the growing spots of the new flux region and the adjacent decaying sunspots and is thus a prime example of an evolving magnetic feature.

In Figure 3 the actual sites of flares occurring between 1500 on 21 June and 0100 on 22 June are shown as dark gray areas superposed on a set of isogauss contours from Kitt Peak Observatory magnetograms. Positive polarity contour lines are wider than negative polarity contour lines. The flares are shown for intervals within 2 hours or less of the time that the magnetograms were acquired. For comparison with the flare locations, the approximate boundary of the new flux region is shown by the dashed contour on the last magnetogram as in Figure 1. Figure 3 illustrates the tendency for most of the flares to cluster around the border of the new flux region. However, we note that the sites of flares that occurred during this interval were definitely not all confined to the key flare sites on the boundary of the new flux region shown in Figure 1.

In Figures 4 and 5, we compare a flare that occurs at key flare site S_1, the evolving magnetic feature, to a subsequent flare that occurs around the old polarity inversion line to the southeast of the new flux region, not an evolving magnetic feature (lower left in Figures 1 and 4). In Figure 4 the brightest flare segments are seen to begin below the sunspot at site S_1. As the flare grows, additional flare points that have appeared within the new flux region (1859:44) are complemented by additional flare points approximately equidistant from S_1 but to the southeast of S_1. Finally, we note a third stage of the flare at 1911:03 in which complementary flare segments appear in opposite polarity fields at the extreme right and left sides of this image and the subsequent images. These outermost parts of the flare are also approximately equidistant from the initial flare site. The pattern of flare development suggests that the conjugate pairs of successive flare elements seen here in the chromosphere should be connected by successively longer and higher flare loops in the corona.

Within 5 hours of the occurrence of the flare in Figure 4, an importance 2 flare takes place at some but not all of the same chromospheric sites. This next flare, shown in

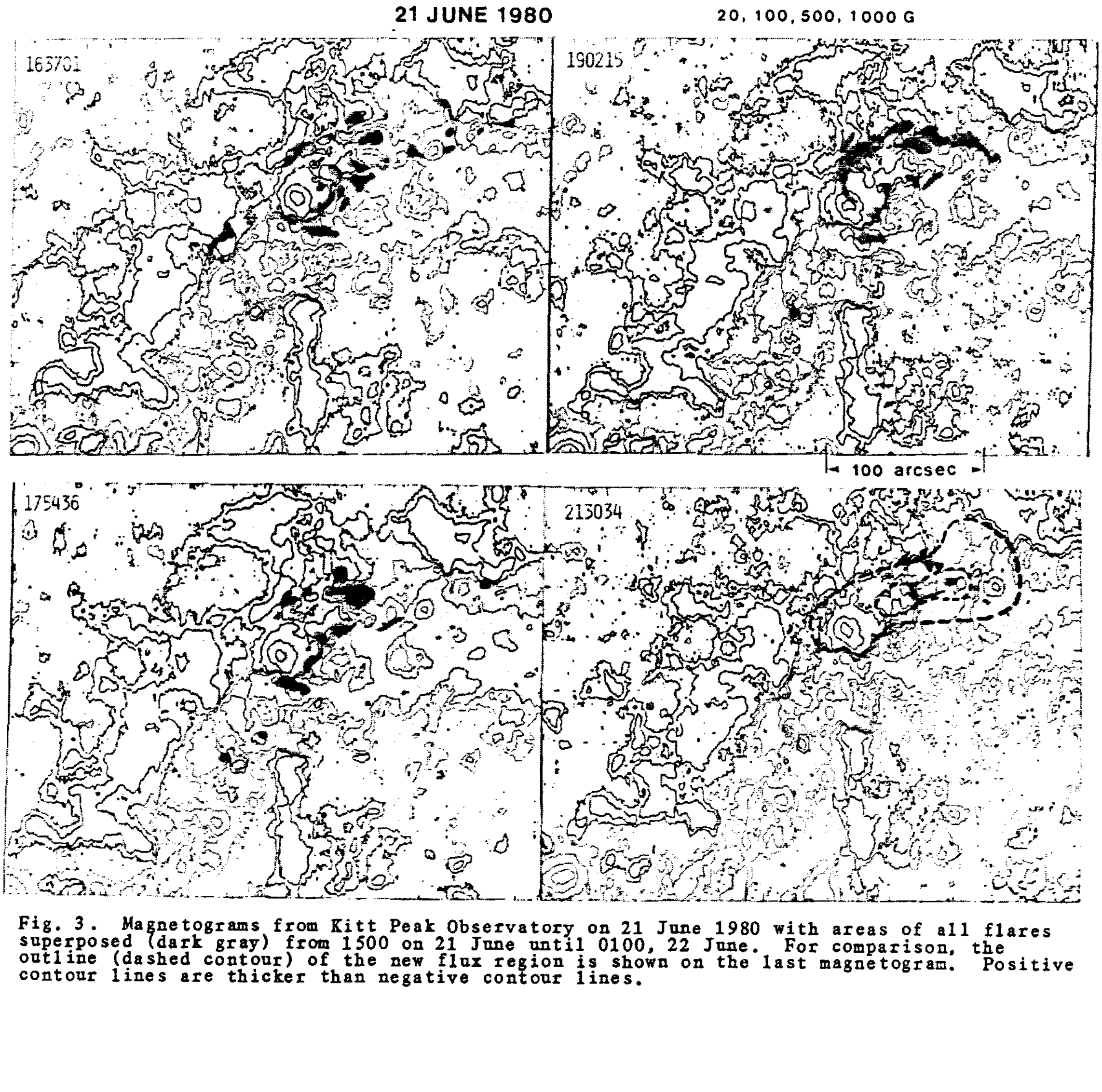

Fig. 3. Magnetograms from Kitt Peak Observatory on 21 June 1980 with areas of all flares superposed (dark gray) from 1500 on 21 June until 0100, 22 June. For comparison, the outline (dashed contour) of the new flux region is shown on the last magnetogram. Positive contour lines are thicker than negative contour lines.

Figure 5, does not display homology with the earlier flare in the sense of starting at the same site. Instead it is seen to begin along the polarity inversion line of the old field to the southeast of the new flux region. It spreads in both directions along the polarity inversion line to form a major classic two ribbon flare. In Figure 5, the contours within the square represent soft X-ray emission detected by the flat crystal spectrometer (FCS) of the X-Ray Polychromator (XRP) aboard the Solar Maximum Mission (SMM) satellite. The highest contours in the soft X-ray images are initially centered over the new magnetic flux region but later appear over the polarity inversion line of the old pre-existing active region. Because long-lived X-ray sources often persist for hours after at least some flares, we think that the early peak in the soft X-ray image should be associated with the remnants of at least one earlier soft X-ray flare and that the lesser peaks in the X-ray flux to the southeast are the ones that should be identified with the start of this major flare on 21 June.

The alignment of the FCS and Hα images from Big Bear Solar Observatory was achieved through the superposition of sunspots in both types of images. The alignment is shown in the upper two images in Figure 5. The dashed contours represent the sunspots in the FCS images. The

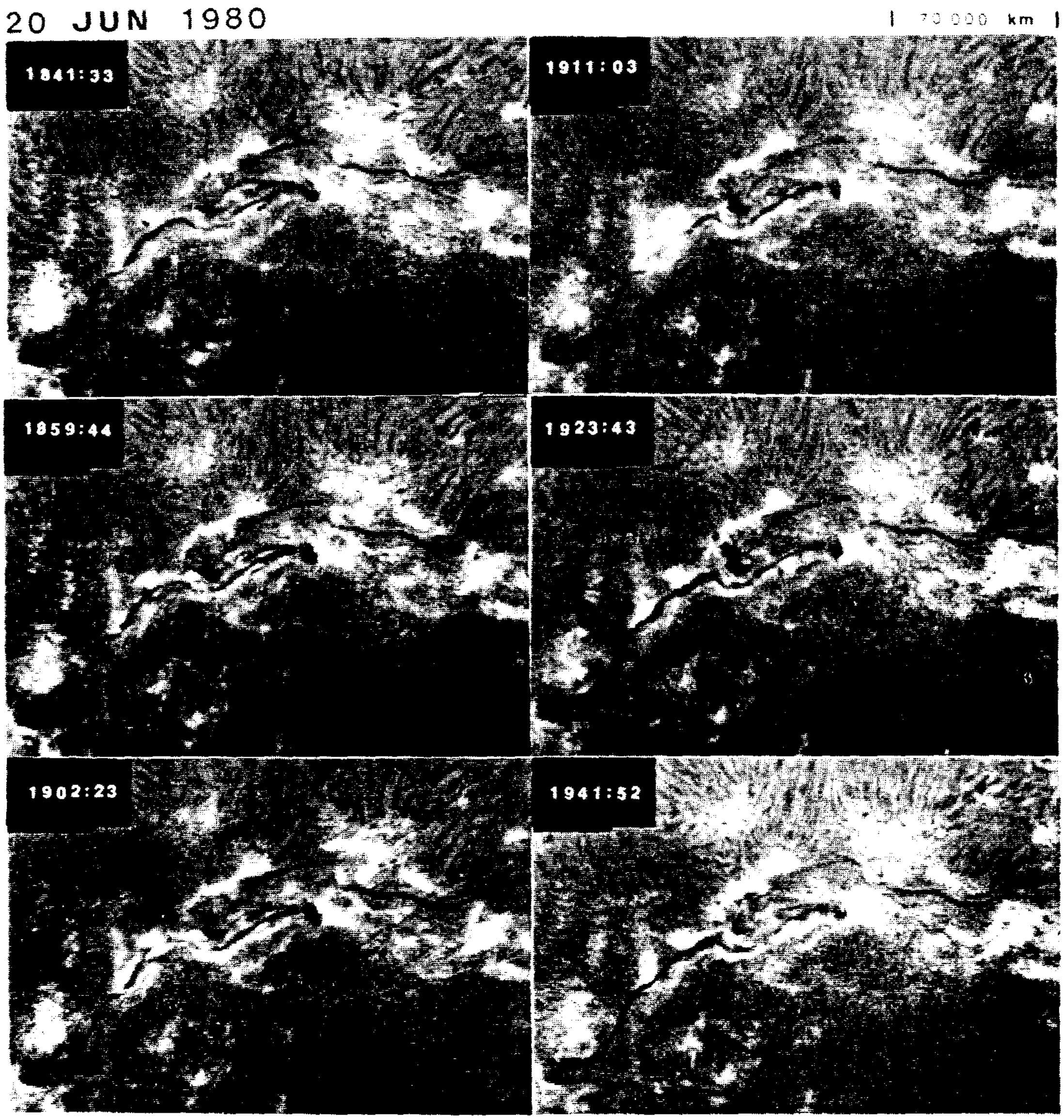

Fig. 4. This flare starts at key flare site S_1 (Figure 1) and spreads nearly symmetrically in time to progressively equidistant sites from S_1. By 1911:03 the flare has spread to the extreme sides of the active region complex. This late flare emission is relatively low in intensity. The pattern of development of the flare in the chromosphere would be consistent with the successive excitation of coronal flare loops at increasing heights above S_1.

FCS sunspots are superposed on images at Hα + 1.0 Å. This alignment can then be transferred to the Hα centerline images for comparisons of the flare emission by first aligning Hα features common between the 1A (upper row) and 1/2A (middle row) and then between the 1/2A (middle row) and Hα centerline images (lower row). Since the field of HXIS (outer box with indented corners) is also known relative to the FCS and XRP field, it is then possible to align the HXIS and Hα images accurately.

The correspondence between the Hα flare ribbons and the HXIS X-rays in the lowest energy band is shown in Figure 6 for three successive times during the 21 June major flare. The peak of the HXIS X-rays coincides well with the XRP X-rays. Since there is only a single dominant peak in all of the X-ray images and the peak straddles the flare ribbons in Hα, we

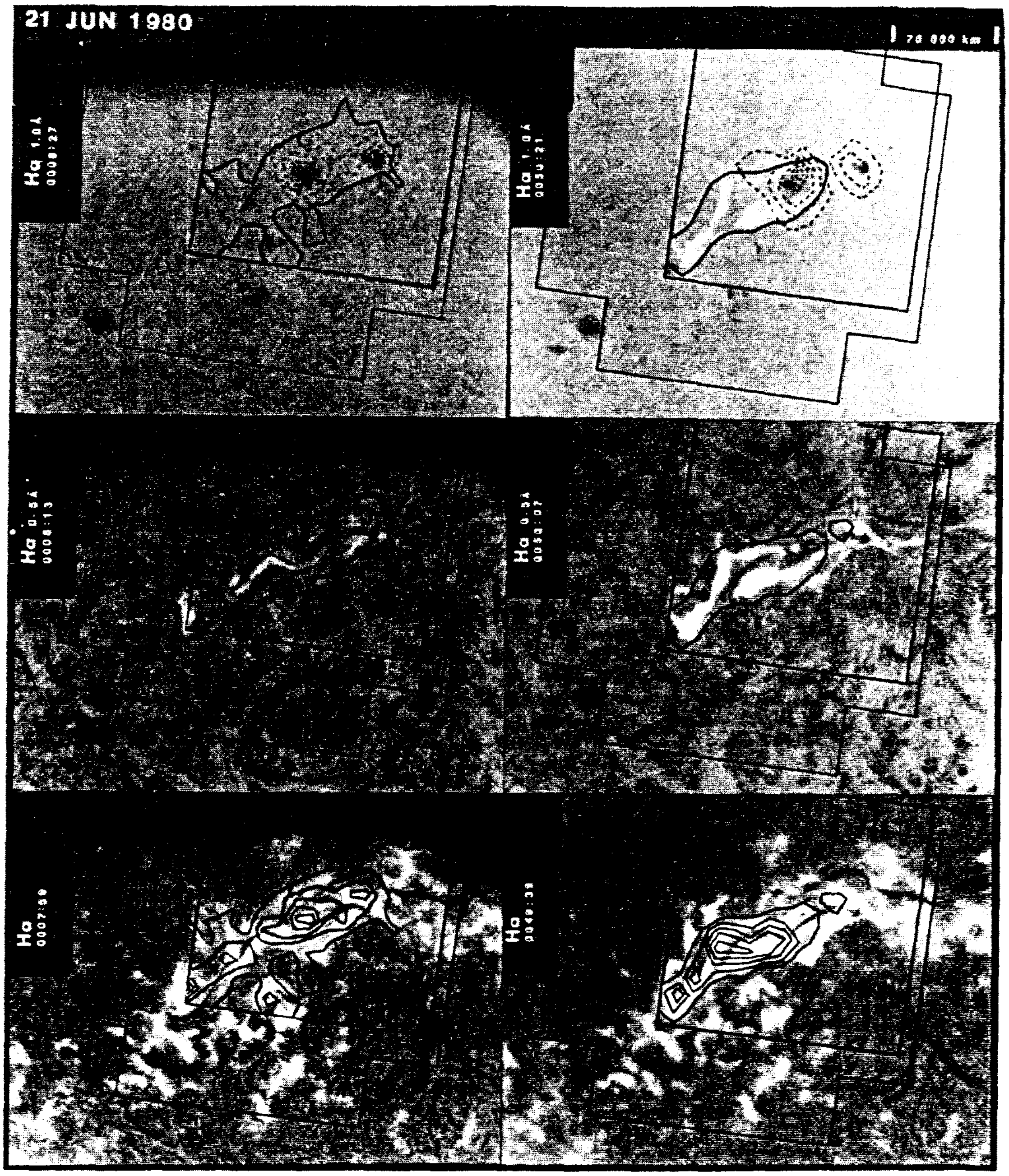

Fig. 5. X-ray contours (solid curved lines) are shown superposed on Hα images from the San Fernando Observatory at 3 wavelengths at the start of the flare (column 1) and during the rise of the flare to maximum (column 2). The relative positions of the soft X-rays from XRP on the SMM satellite and the flare in Hα was found by aligning the sunspots recorded both in XRP (FCS images) and in the wings of Hα (top row) Hα + 1.0 Å. This alignment is then transfered to Hα + 0.5 Å (middle row) on to Hα centerline images (lower row). The soft X-rays are seen to center over the polarity inversion line between the flare ribbons in Hα.

conclude that the X-ray emissions are dominantly coming from a loop system overlying the polarity inversion line. An Hα loop system was subsequently observed during the later phase of the event in Hα. Both the chromospheric and coronal data sets confirm our assertion that this major flare did not start at any of the key flare sites along the boundary of the emerging flux region.

Less than one day after the large flare on 21 June, illustrated in Figures 5 and 6, another substantial flare did occur exactly on the boundary of the new flux region. This flare, beginning at 1910, is shown in Figure 7. The flare starts at key flare site S_4, (Figure 1) where relatively bright opposite polarity plage is very close together and filaments extend in both directions from this site. The Hα flare develops in opposite directions from the key flare site in such a way that it can be imagined to be the footpoints of flare loops that are excited at successively higher points in the corona, but still centered approximately vertically above the key flare site. This flare is regarded as a primary consequence of the growth of the new flux which plays a key role in the build-up of the circumstances for the flare to occur.

The next major flare to occur in this complex grew to encompass the same flare site as in Figure 7 but was initiated at the key flare site S_3, further west along the same polarity inversion line. This flare is illustrated in Figure 8 along with a diagram made at the

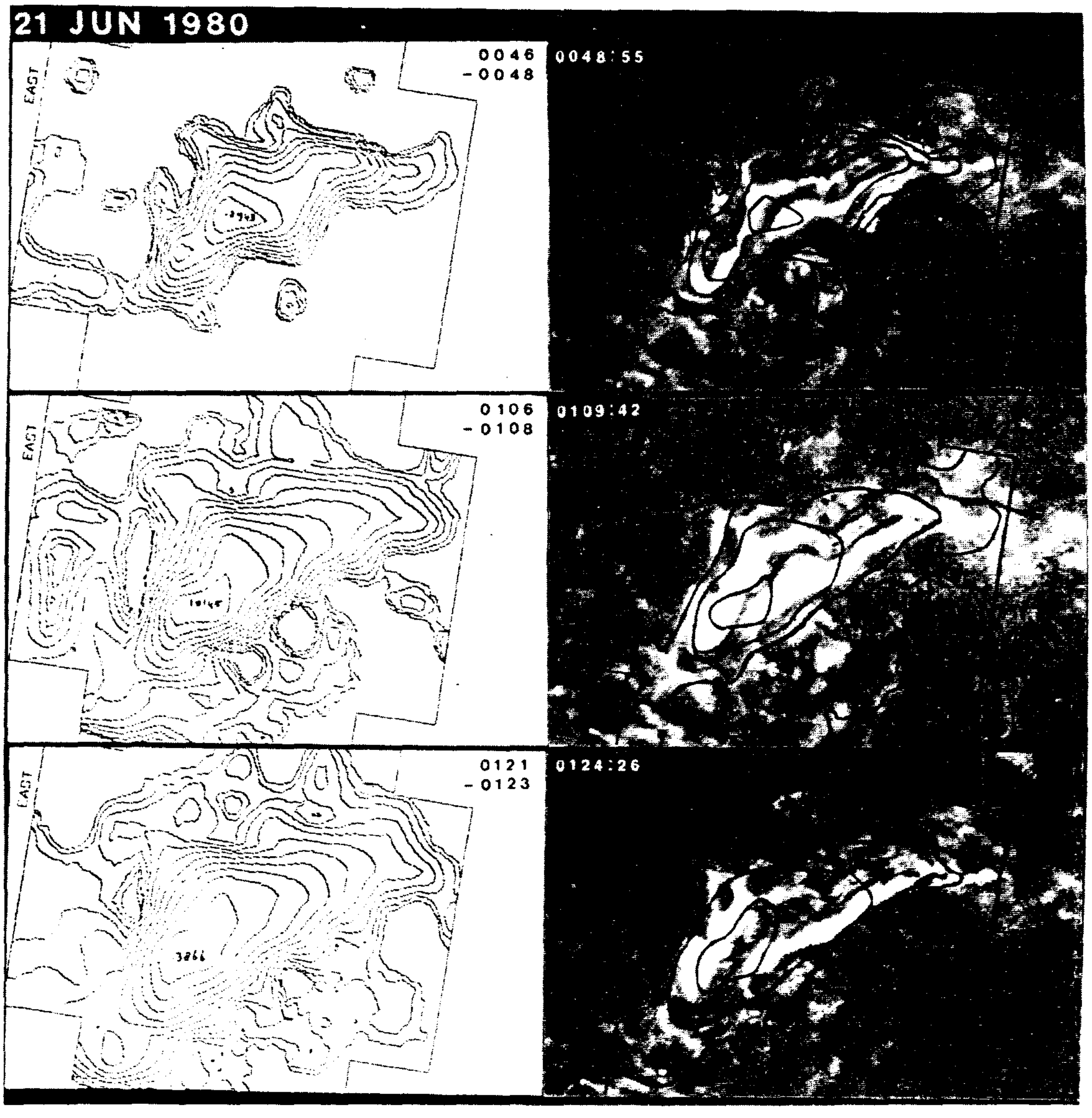

Fig. 6. Soft X-rays from the HXIS lowest energy band are shown relative to the flare ribbons in Hα. The alignment was achieved as in Figure 5 with the additional knowledge of the position of the HXIS field relative to the XRP field also shown in Figure 5. A single peak in the HXIS X-rays is also centered over the polarity inversion line between the flare ribbons but southeast of the major new flux region.

Debrecen Observatory that shows the previous and subsequent positions of the closest sunspot of the emerging flux region. Figure 8 also shows the previous and subsequent positions of the filament at and near the flare site.

In order for the sunspot illustrated in Figure 8 to move approximately parallel to the neutral line, the spot must push outlying flux of similar polarity toward the key flare site. Due to this westward motion, we also expect the gradient of the magnetic field to be increasing - at least until about midday on 22 June after which time the spot area is seen to decrease. The increasing gradients at this key flare site and the key site of the 21 June, 1910 flare are confirmed in the series of 62 area scan magnetograms acquired at Kitt

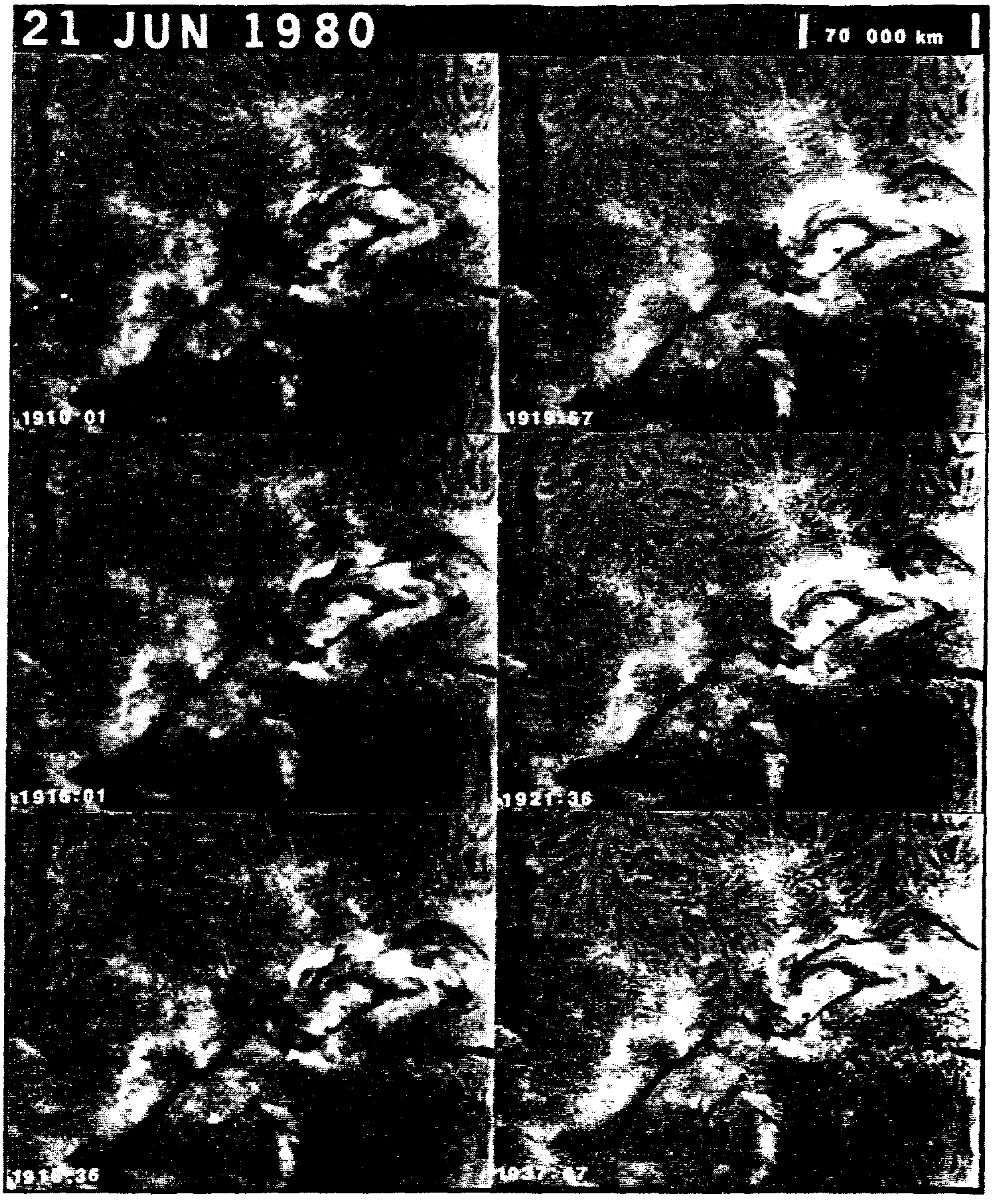

Fig. 7. This flare beginning at 1910:01 coincides with key flare site S_4 (Figure 1). It spreads progressively along the boundary of the new flux region until it reaches the dominant opposite polarity sunspots. This flare, like the one in Figure 4, develops in a symmetrical pattern with successive chromospheric elements forming at nearly equidistant locations with respect to the key flare site. This pattern would be consistent with the successive excitation of coronal flare loops at progressively higher altitudes above the key flare site as a function of time.

Peak Observatory on 21 June. From the earliest magnetogram at 1637 until the flare at 1910, the gradient close to the polarity inversion line is building up as opposite polarity peaks of magnetic field come closer together. Due to minor distortions from data line to data line in the magnetograms we are not yet certain whether the gradient continues to increase during the flare at 1910. However, after this flare it is clear that the opposite polarity peaks in the field continue to move closer together. In addition, the length of opposite polarity contact along the inversion line is increasing. The negative polarity moves toward and into the weaker parts of positive polarity field. These changes are related to the westward migration of the leading polarity, negative sunspot of the new flux region as shown in Figure 8. Less than 13 hours after the last magnetogram at 2323 on 21 June, the major flare on June 22 began.

DISCUSSION AND CONCLUSIONS

We have found that the flares in this complex have differing relationships to the growth of a new major flux region. The flares having the closest relationship to the new flux region are those that straddle the boundary between the new and pre-existing magnetic flux regions. The flares at 1859 on 20 June (Figure 4) and 1910 on 21 June (Figure 7) are of this type. Another group of flares originate at sites west of the emerging flux region

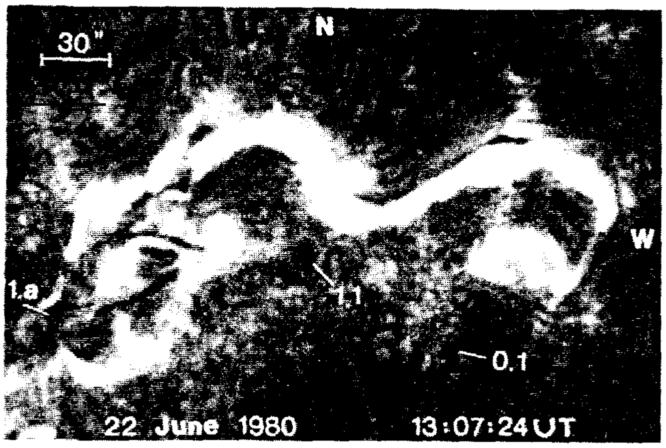

(Debrecen Observatory filtergram.)

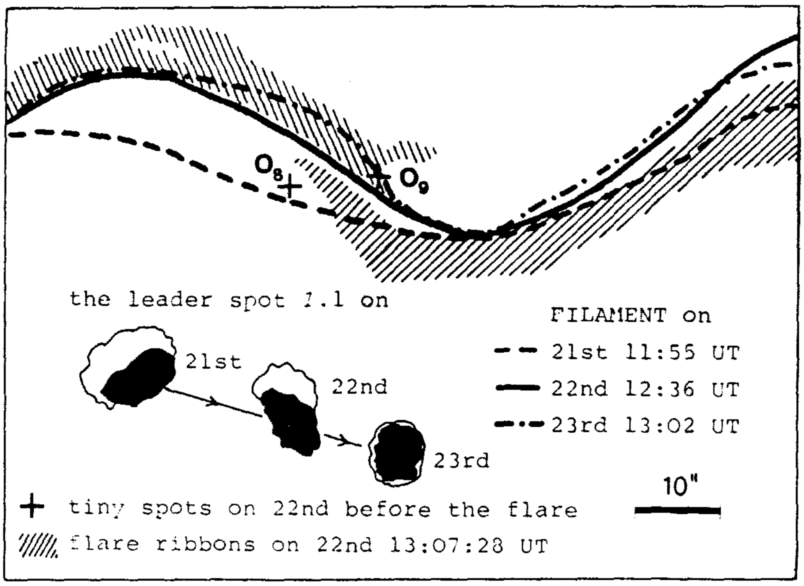

Fig. 8. Motions of the leader sunspot within the major new flux region and changes in the position of the neighboring polarity inversion line (filament) are shown prior to and after the major flare on 22 June 1980. The diagram, made at the Debrecen Observatory, corresponds to the central part of the filtergram on the top. The initiation site of this flare is centered at the place where the filament position was fixed during this 3 day interval. This site is identified as key flare site S_3 in Figure 1.

where the relatively rapid motion of the leading polarity field (Figure 2) pushes the pre-existing field of similar polarity towards an opposite polarity field. The 22 June flare (Figure 8) is among this group of flares. The major flare on 21 June does not fit either of the above categories. There is little motion of the trailing sunspots toward the old polarity inversion line around which the flare begins. However, the magnetic field configuration suggests that magnetic reconnection could readily occur between the positive field associated with the trailing sunspots of the emerging flux region and the adjacent negative polarity pre-existing field. This offers a third possible relationship to the new flux region. If the trailing, positive polarity fields of the new flux region slowly or intermittently reconnect with the negative fields of the old region, this reconnection would effectively "steal" old flux previously connected to its conjugate field over the adjacent old polarity inversion line. As the previous magnetic configuration changes, the filament along the old polarity inversion line reacts and begins to ascend into the corona. Finally the magnetic configuration in the corona changes from metastable to unstable and the flare occurs. Although we lack data to show direct evidence of such changes in the coronal magnetic field, we suggest that many flares associated with erupting filaments or "disparition brusques" occur as in this last scenario. As evidence of this third relationship, we cite the unusually high incidence of disparition brusques in the vicinity of new and growing active regions found by Bruzek/7/ and confirmed by Hermans and Martin/12/.

Although the emerging flux region described here had affected the flare productivity of the complex in these several ways described, we do not claim that all emerging flux regions are effective in generating the conditions necessary for flares. Especially when the rate of growth of a new emerging flux region is slow or the orientation is such that similar polarities of new and old flux can merge, we would not expect flares to occur. Additionally, we think that it is feasible for flare conditions to be generated in the absence of emerging flux.

ACKNOWLEDGEMENTS

The acquisition of filtergrams by Big Bear Solar Observatory was made possible by NASA grant 05-002-034 and NSF grant ATM-7911139. KLH acknowledges support under NSF grant ATM-8319589. The contribution of SFM was supported by AFOSR grant 82-0018.

REFERENCES

1. V. Gaizauskas, SMM Workshop on Solar Flares, to be published by NASA, USA.

2. E. Priest, SMM Workshop on Solar Flares, to be published by NASA, USA.

3. S.F. Martin, L. Dezso, A. Antalova, A. Kucera, and K.L. Harvey, Adv. Space Res., 2, 39-51 (1983).

4. J. Athay, H. Jones, and H. Zirin, submitted to Astrophys. J. (1984).

5. V. Gaizauskas, Adv. Space Res., 2 (1983).

6. A. Bruzek, Solar Phys., 2, 451 (1967).

7. A. Bruzek, Zeit Astrophys., 31, 199 (1952).

8. S. Weart, Astrophys. J., 177, 271 (1972).

9. V. Bumba, L. Krivsky, M.J. Martres, and I. Soru-Iscovici, IAU Symp., 35, 311 (1968).

10. M.J. Martres, R. Michard, I. Soru-Iscovici, and T. Tsap, IAU Symp., 35, 318 (1968).

11. M.J. Martres, R. Michard, I. Soru-Iscovici, and T. Tsap, Solar Phys., 5, 187 (1968).

12. L.M. Hermans and S.F. Martin, Proceedings of the Workshop on Solar Terrestrial Predictions, Observatory of Paris at Meudon, 18-22 June 1984.